SCIENTIFIC REPORTS

OPEN

SUBJECT AREAS:
PHOTOCATALYSIS
NANOPARTICLES

Received
8 October 2013

Accepted
20 March 2014

Published
4 April 2014

Correspondence and requests for materials should be addressed to X.Y.Z. (xyzhang@ysu.edu.cn); J.Q.Q. (jiaqianqin@gmail.com) or R.P.L. (riping@ysu.edu.cn)

* These authors contributed equally to this work.

Effect of aspect ratio and surface defects on the photocatalytic activity of ZnO nanorods

Xinyu Zhang[1]*, Jiaqian Qin[2]*, Yanan Xue[1], Pengfei Yu[1], Bing Zhang[1], Limin Wang[1] & Riping Liu[1]

[1]State Key Laboratory of Metastable Materials Science and Technology, Yanshan University, Qinhuangdao 066004, P. R. China, [2]Metallurgy and Materials Science Research Institute, Chulalongkorn University, Bangkok 10330, Thailand.

ZnO, aside from TiO_2, has been considered as a promising material for purification and disinfection of water and air, and remediation of hazardous waste, owing to its high activity, environment-friendly feature and lower cost. However, their poor visible light utilization greatly limited their practical applications. Herein, we demonstrate the fabrication of different aspect ratios of the ZnO nanorods with surface defects by mechanical-assisted thermal decomposition method. The experiments revealed that ZnO nanorods with higher aspect ratio and surface defects show significantly higher photocatalytic performances.

Metal oxide, mixed oxide, and hybrid noble-metal/oxide nanocrystals (NCs) have great potential for electronic, magnetic, optical, and photocatalytic applications[1–3]. In particular, ZnO is an important group II–VI semiconductor with a wide band gap (3.37 eV) and a large exciton binding energy of 60 meV at room temperature[4]. ZnO, aside from TiO_2, has been considered as a promising material for purification and disinfection of water and air, and remediation of hazardous waste, owing to its high activity, environment-friendly feature and lower cost[5–7]. Previous studies have proved that ZnO can degrade most kinds of persistent organic pollutants, such as detergents, dyes, pesticides and volatile organic compounds, under UV-irradiation[5–7]. Actually, the disadvantage of ZnO is that it absorbs only in the UV region because of its large bandwidth of 3.2 eV ($\lambda = 380$ nm). The major problem is that only about 4 to 5% of solar spectrum falls in the UV range. Therefore, the effective use of solar energy still remains a challenge in photocatalytic application.

Several efforts have been made to enhance the photocatalytic activity of ZnO by tailoring size[8], concentration of oxygen defects[9,10], facets[11–13], and surface area[14,15]. Recently, Jang et al. and McLaren et al. have reported the relationship between the exposed surfaces of ZnO crystals and their photocatalytic efficiency, and demonstrated that a greater proporation of exposed polar surfaces leads to a greater photocatalytic activity[12,16]. They discovered that OH^- ions prefer to adsorb onto (0001)-Zn surface due to its surface positive charge, which can react with hole (h^+) to generate reactive species ·OH radicals, hence enhancing the photocatalytic activity[17]. The amount of e^-/h^+ on the photocatalyst surface is a key factor in determining the photocatalytic reaction rate. One-dimensional (1-D) ZnO nanostructures such as nanorods and nanowires have been investigated extensively due to their superior electrochemical properties, which are attributed to dimensional anisotropy. Consequently, larger number of e^- and h^+ exist on the active sites of the nanocrystal surface, resulting in higher activity compared with spherical nanoparticles.

Besides the exposed crystal facet and aspect ratio, the surface defects on ZnO are another very important factor influencing its photocatalytic performance. In fact, the defects on ZnO have been extensively characterized by various techniques, and their roles in adsorption and surface reactivity have been acknowledged[18–20]. Zheng et al.[20] showed that different oxygen defects (oxygen vacancies and interstitial oxygen) that formed in a solvothermal process had an impact on the photocatalytic activity of ZnO. Wang et al.[18] developed enhanced the visible light photocatalytic activity of ZnO by narrowing the band gap with defects. Li et al.[21] reported that tuning the relative concentration ratio of bulk defects to surface defects in TiO_2 nanocrystals can improve the separation of photo-generated electro-hole and therefore can enhance photocatalytic efficiency. However, it is still challenging to major problem is that the defects are interacting with many other factors and the photocatalytic activity is dominated by the balance among all these factors. One should bear in mind that defects exist in most ZnO samples except perfect single crystals, and the degree of defects may differ a lot in different samples. Therefore, it is difficult to study the effects from other factors, e.g. crystalline phases and exposed crystal facets, while it is rational to investigate the sole effect of defects on the photocatalytic activity of ZnO, providing that other factors could be

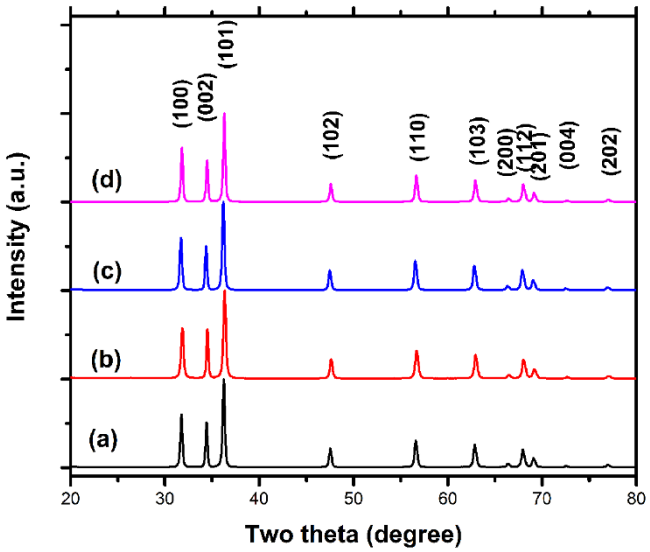

Figure 1 | **XRD patterns of as-synthesized ZnO under calcination temperature of (a) 350°C, (b) 400°C, (c) 450°C, (d) 500°C.**

kept unchanged. According to previous study, Lin et al. developed the thermal decomposition method from zinc acetate dihydrate[22], which is a simple, cost effective, and rapid synthesis route. Now researchers did many ZnO studies by using this method[23–25]. Here ZnO nanostructures with various aspect ratios and defects were synthesized by a mechanical-assisted thermal decomposition method. We demonstrate that thermal decomposition is a successful and general procedure to control the aspect ratio, the pre-grinding process can make the sawtooth-shaped side plane of ZnO nanorods, and so the different temperature and pre-grinding process could adjust the surface defects. With all the other influencing factors strictly restricted, surface defects could play a very important role in the photocatalytic activity hence the high aspect ratio of ZnO nanorods with surface defects is responsible for the higher photocatalytic activity under high pressure sodium lamp irradiation.

Results

The synthesis was based on the modified method by Lin et al.[22] with mechanical assisted. X-ray diffraction (XRD) data (Figure 1) confirmed that all of the samples produced were crystalline and had the hexagonal wurtzite structure of bulk ZnO lattice parameters matching those in the literature. It was found that an increase in the calcinations temperature led to an increase in the average particle sizes according to the field emission scanning electron microscopy (FESEM) and transmission electron microscopy (TEM) results (Figure 2 and Figure 3). Figure 2 (a) gives the FE-SEM image of ZnO calcined at 350°C and shows the nanorods shape of ZnO. As seen in Figure 2 (a), the length is about 800 nm, and diameter is about 30–50 nm. When the temperature was raised to 400°C and 450°C, the image (Figure 2(b) and (c)) indicates the nanorods with increase in diameter and decrease in length. Further, the rise in temperature to 500°C represents that large amount of ZnO is irregular particles (average size ~100 nm) (Figure 2 (d)), but there are still some nanorods shape particles (~100 nm in diameter, ~200 nm in length). As the calcinations temperature increases, the particle morphology changes from rod to irregular shape. This anisotropic growth on ZnO particles could be caused by higher temperature. Therefore, the SEM images implied that the calcinations temperature is one of the role factors to affect the surface morphology.

The morphologies of ZnO crystallites and particles were also investigated by TEM. Figure 3 shows typical low-magnification TEM images of the synthesized ZnO under the calcinations temperature of 350°C and 500°C. Figure 3(a), (b) and (c) indicate that most of the nanorods have straight sides and regular ends. When the temperature was raised to 500°C, the particle morphology changes from rod to irregular shape (Figure 3(d)). The average length of nanorods is ~800 nm, and the diameter is ~30–50 nm at calcination temperature of 350°C. With the calcinations temperature increasing, it is seen that the nanorods with increase in diameter and decrease in length. Further, the rise in temperature to 500°C represents that the ZnO is irregular particles (average size ~100 nm). These TEM results are in good agreement with the FE-SEM observations.

We also examined the crystallographic nature of the individual ZnO nanorod and ZnO irregular particles using high-resolution

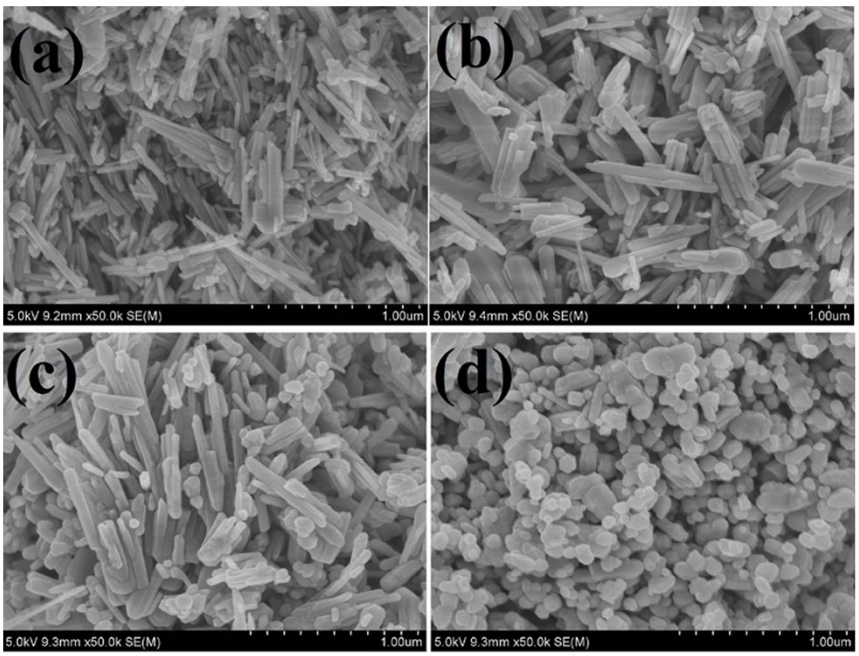

Figure 2 | **FE-SEM images of as-synthesized ZnO under temperature of (a) 350°C, (b) 400°C, (c) 450°C, (d) 500°C.**

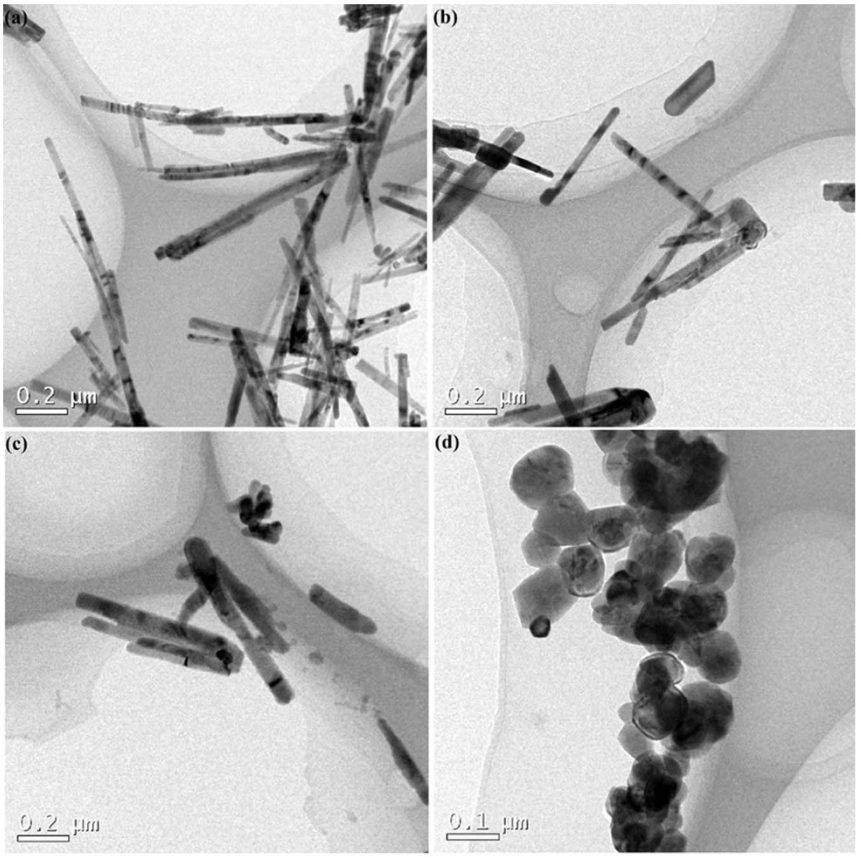

Figure 3 | **TEM images of as-synthesized ZnO under temperature of (a) 350°C, (b) 400°C, (c) 450°C, (d) 500°C.**

transmission electron microscopy (HRTEM) observations and selected area electron diffraction (SAED). Figure 4 gives the HRTEM and the insets of small image show the SAED and the selected area of TEM image. As seen in Figure 4, HRTEM images of rod shape ZnO nanoparticle synthesized under 350°C, 400°C, and 450°C show well ordered crystalline planes with a spacing of 0.523 nm, corresponding to the (0001) planes of ZnO. Therefore, it is a section of ZnO nanorod in the [001] orientation, showing the growth direction as [001]. As seen in Figure 4(d), the HRTEM and SAED also reveal that the irregular particle is a section of ZnO short rod shape in the [001] orientation, implying the growth direction as [001] and side planes, e.g., (10-10), (01-10), (1-100) and (-1100) planes, as shown in Figure 5(a). It is seen that side planes are saw-tooth-shape surface from the HRTEM image. The HRTEM image and SAED pattern for a hexagonal nanocrystals indicate a single-crystalline structure with interplanar *d*-spacing of *ca.* 0.523 nm for ZnO nanocrystal under different calcination temperature, which is attributed to the (0001) planes of ZnO crystals, indicating preferential growth along the [001] direction, as confirmed by the SAED pattern of the [0–10] zone-axis. Taking all these TEM images into

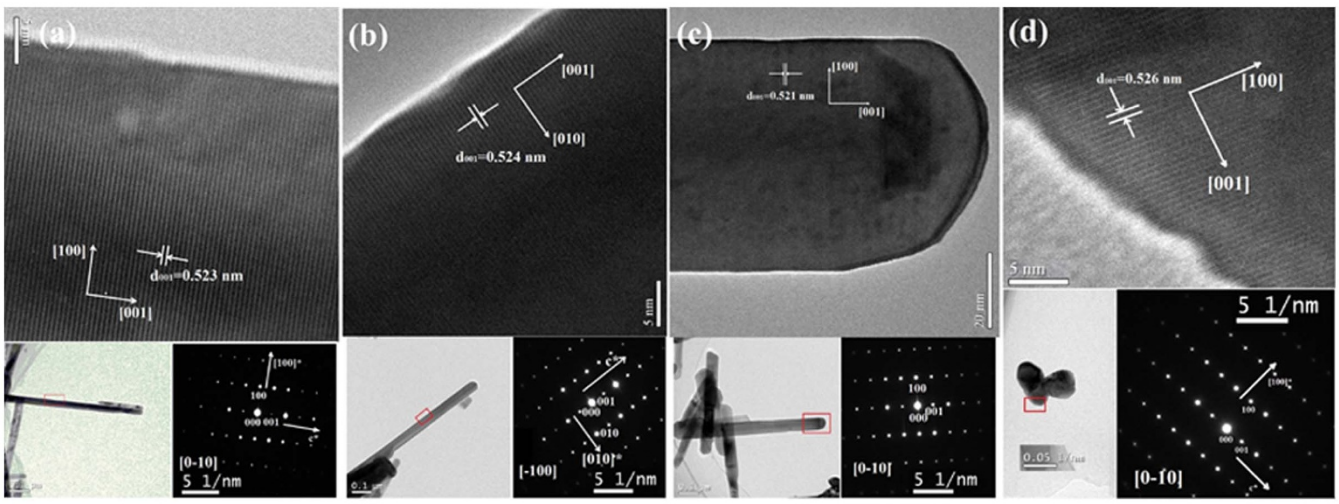

Figure 4 | **HRTEM of as-synthesized ZnO under temperature of (a) 350°C, (b) 400°C, (c) 450°C, (d) 500°C.** The insets of small image show the SAED and the selected area of TEM image.

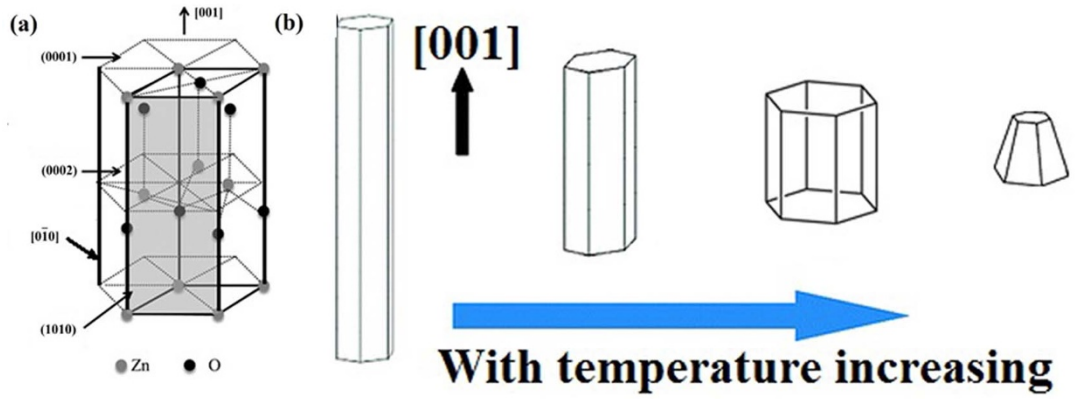

Figure 5 | (a) Shape of the nanorod. Note, [uvw] is an index of a specified crystal axis and (hkil) is an index of a specified crystal plane. (b) Schematics of nanorods growth with increasing temperature.

account, the real shape, crystal structure and growth schematic of the nanorods could be approximately re-constructed, as shown in Figure 5(a), in which the axial direction is [001]. The synthesis mechanics of ZnO has been discussed by Lin et al.[22], in the current study, the fracture of ZnO nanorods and growth in diameter will be occurred with increasing temperature (Figure 5(b)).

UV-visible spectra (Figure 6) of the as-synthesized ZnO at different temperature imply that temperature can play the role in changing the absorption characteristics of ZnO. Strong absorption band in UV region at 373 nm attributed to the band edge absorption of wurtzite hexagonal ZnO, blue shift relative to its bulk (380 nm)[26]. The absorption band is increased with annealing temperature increasing. As seen in Figure 6, the absorption band is 379 nm at 500°C, which is similar to that of bulk ZnO[26]. The blue shift denotes the decrease in size of particle and increase in band gap energy. The band gap energy (E_{bg}) of ZnO can be calculated from the following equation, $E_{bg} = 1240/\lambda$ (eV)[27–29], E_{bg} is the bandgap energy in eV and λ is the wavelength in nanometers. The bandgap values of ZnO are 3.32 eV, 3.30 eV, 3.30 eV, and 3.27 eV, for the calcination temperature of 350°C, 400°C, 450°C, and 500°C, respectively. The corresponding wavelength of bandgap values exists in the UV region. Considering large surface area resulting from the rod-like ZnO particles may exhibit good photocatalytic ability for dye degradation, and the theoretical study shows that (0001) surface has the highest photocatalytic activity and a remarkable red-shift phenomenon of the absorption edge[30]. Here the photodegration of methylene blue (MB) experiments were performed under high-pressure sodium lamp. Figure 7(a) shows photodegradation efficiency of MB using 350 as photocatalyst. It is clearly seen that the change in concentration of MB by ZnO nanorods catalyst under high-pressure sodium lamp irradiation for different time intervals. As seen in Figure 7(a), a gradual decrease in the intensity of strong absorption band at 664 nm for MB solution is observed during the course of the photo-assisted degradation, indicating that the large chromosphere group of MB dye molecule, i.e., the conjugated π system, has been destroyed[31,32]. The above result confirms that the oxidative decomposition of MB molecule has occurred.

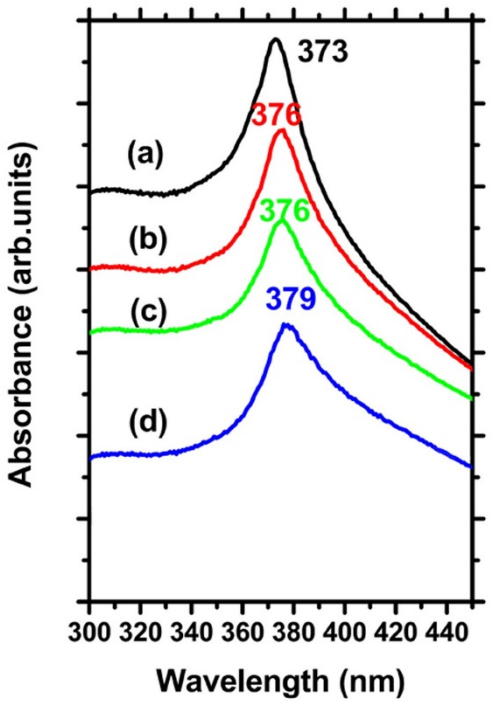

Figure 6 | **UV-visible spectra of the as-synthesized ZnO at different temperature of (a) 350°C, (b) 400°C, (c) 450°C, (d) 500°C.**

The dependence of MB photo degradation on the different samples was also investigated at the same operating conditions. The results are shown in Figure 7(a). When the suspensions were magnetically stirred in the dark for 2 hours to ensure establishment of an adsorption/desorption equilibrium of MB on the sample surface, the MB solution concentration decreased only a little because of the adsorption. As shown in Figure 7(a), after the high-pressure sodium lamp turned on, sample 350 exhibits higher photocatalytic activity than other samples. The degradation percentages after 80 min over 350, 400, 450, and 500 samples are 99.3%, 88.1%, 86.0%, and 56.9%, respectively, which clearly shows that the longer nanorods show a higher activity as compared to the shorter rods. The photocatalytic stability of 350 sample was also carried out for 80 min. As shown in Figure 7(b), the degradation of 350 sample shows no visible change after five recycles. It reveals that 350 sample has a good reusability performance.

The surface and sub-surface components and oxidation states of ZnO prepared at different annealed temperature were investigated by XPS analysis. The O 1s spectra from the nanorods are shown in Figure 8. XPS analysis of the nanorods shows asymmetric O 1s spectra from the nanorods that can be deconvoluted into three peaks, as shown in Fig. 8. The binding energy values at 530 eV, 531.4 eV, and 532.4 eV are observed in all samples. These peaks are associated with O^{2-} species in the lattice (O_L), oxygen vacancies or defects (O_V) and chemisorbed or dissociated (O_C) oxygen species[33,34]. Since the physically absorbed hydroxyl groups on ZnO can be easily removed under the ultrahigh vacuum condition of the XPS system, ZnO nanorods with fine surface structure will not give significant signals in XPS[35,36]. Therefore, the distinct signals of hydroxyl groups observed should be due to hydroxyl groups, i.e. Zn-OH and

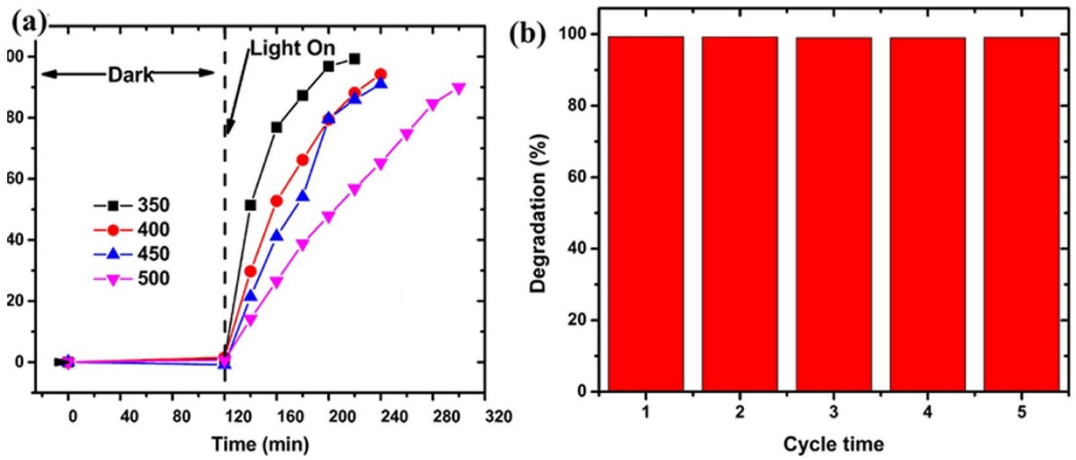

Figure 7 | (a) MB degradation activities of samples 300, 400, 450, and 500. (b) The stability of 350 sample for photodegradation of MB.

H_2O, strongly bound to surface defects on ZnO. That is, the hydroxyl groups in XPS are associated with surface defects and the visible hydroxyl groups should indicate the existence of surface defects on ZnO samples. According to the XPS results, the O_V (531.4 eV) and O_C (532.4 eV) value of O 1s is higher for the high aspect ratio nanorods (Fig. 8), which implies that higher aspect ratio of ZnO nanorods have higher amount of surface defects and the visible hydroxyl groups. Many reports showed that the photocatalytic activity differences among different nanostructures are due to varying oxygen defect concentration and type of defect. Further, oxygen species around 532.4 eV is caused by the surface hydroxyl group. Presence of surface hydroxyl groups facilitates the trapping of photoinduced electrons and holes, thus enhances the photocatalytic degradation process.

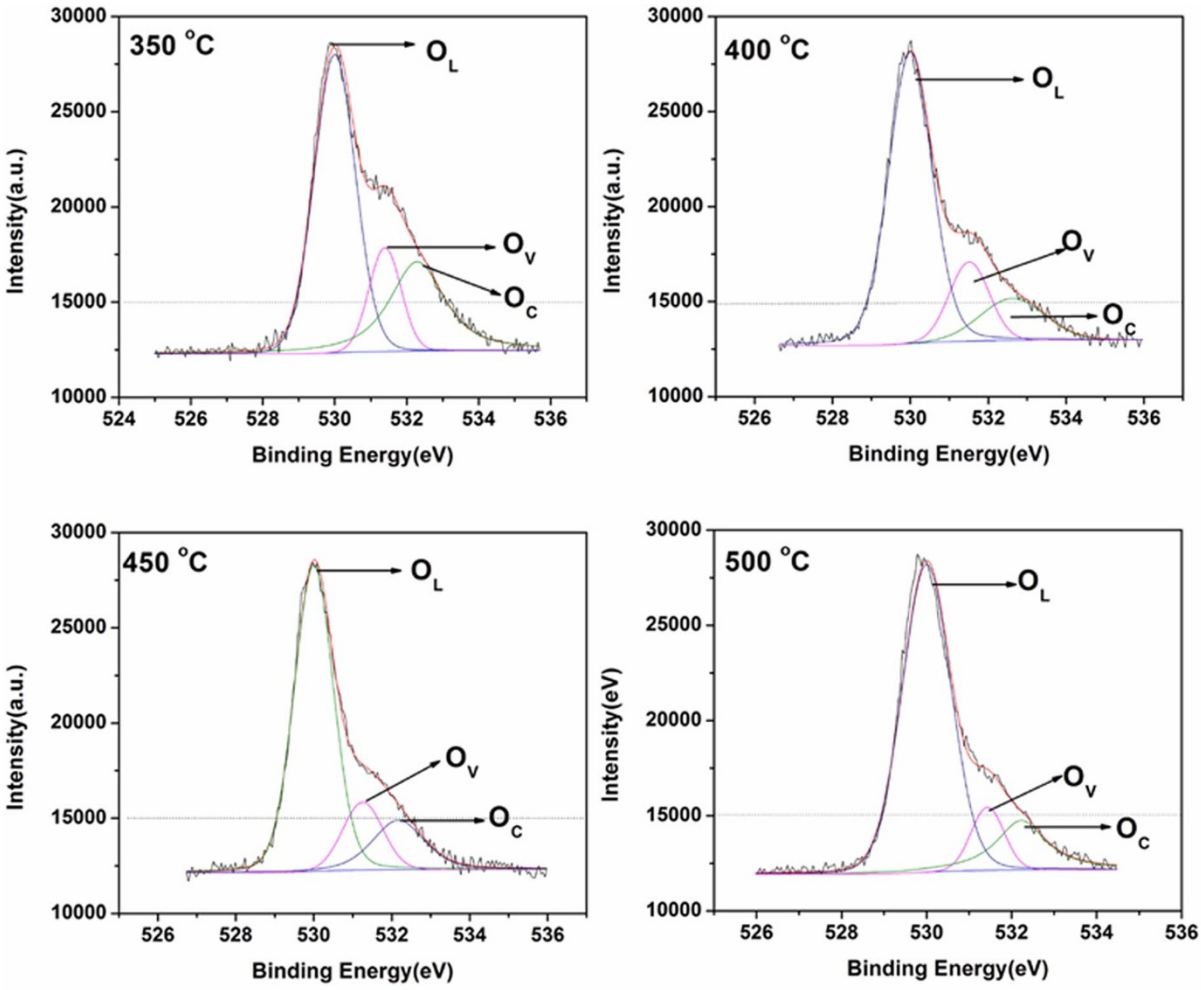

Figure 8 | **XPS analysis, O 1s spectra of different length nanorods indicating the presence of three types of oxygen, O_L (lattice oxygen), O_V (oxygen vacancy or defects) and O_C (chemisorbed oxygen species).**

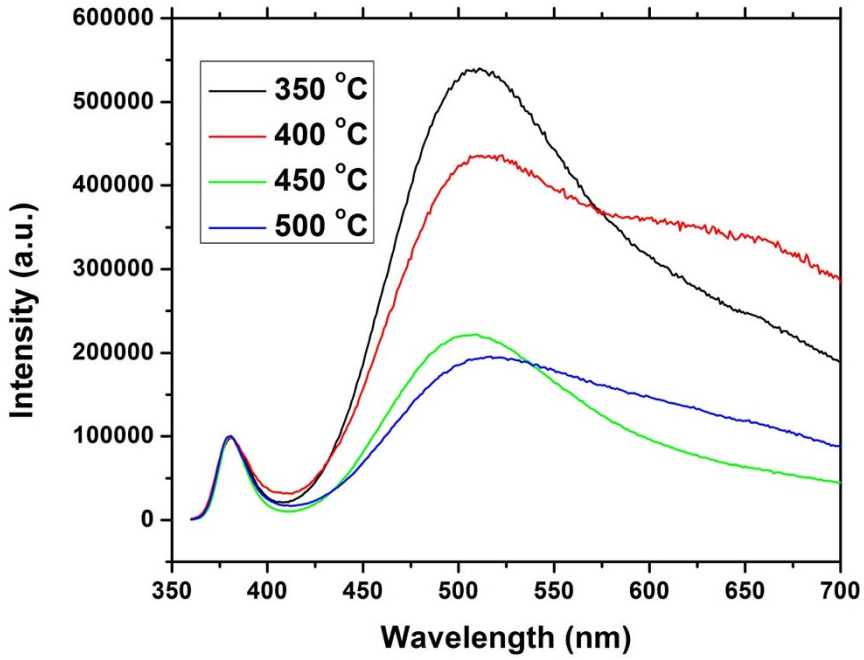

Figure 9 | Photoluminescence spectra of ZnO nanorods prepared at different temperatures.

To confirm the XPS results, we also measured the photoluminescence (PL) spectroscopy of ZnO nanorods prepared at different temperature. PL is a very useful technique to disclose the efficiency of charge carrier trapping, immigration and transfer in a semiconductor[37]. Generally, the photoluminescence emissions on semiconductor materials are originated from the radiative recombination of photo-generated electrons and holes, and two major photo-physical processes can give rise to photoluminescence signals. PL spectra obtained from the samples prepared at different temperatures of 350°C, 400°C, 450°C, and 500°C are shown in Figure 9. PL results show the typical two emissions of narrow violet (~380 nm) and broad green-yellow bands (~510 nm) (Figure 9). To scrutinize the green defect emission (broad band in the visible region), the peaks of the near band edge (NBE) emission in the spectra were normalized to the same value. The broad emission band revealed in the visible region in our samples is due to the superposition of green and yellow emissions. ZnO commonly exhibits luminescence in the visible spectral range due to different intrinsic or extrinsic defects[38]. According to the synthetic process as well as the assignments of defects in the literature discussed above, the defects formed in our system are likely to be due an oxygen vacancy and an interstitial oxygen, corresponding to the green and yellow bands in PL, respectively. The two different oxygen defects are competing with each other, presenting in the competition of green and yellow bands in PL. Two impurity levels, which can enhance the electron hole pair separation rate in ZnO nanorods, are generated in the presence of oxygen vacancies and interstitial oxygen defects. As the redox reactions might occur on the surface of oxygen vacancies and interstitial oxygen defects, the oxygen defects can be considered to be the active sites of the ZnO photocatalyst[39]. As seen in Figure 9, the PL emission intensity decreases with annealing temperature, suggesting the reduction of the oxygen defects in ZnO nanorods, which is consistent with the increase of the oxygen defects of ZnO nanorods with aspect ratio of nanorods. Therefore, the photocatalytic activity of the ZnO nanorods can be enhanced with aspect ratio in the present study. It can be concluded that abundant surface oxygen vacancies or defects exist in ZnO nanorods, which may play a vital role in the photocatalytic activity.

Discussion

The photocatalytic activity of the metal oxides depends on various factors including composition, phase structures, surface hydroxyl groups, particles size, crystalline, surface defects, surface metal deposits, and adsorbates or surface bound complexes. The role of these parameters on the photocatalytic activity of different structures of ZnO is well reported and investigated[40]. In general, the difference in photocatalytic activity is related to size and surface area, the specific surface area of rods are 8.02, 7.85, 7.91, and 6.04 m^2/g respectively for annealed temperature 350°C, 400°C, 450°C, and 500°C. The phtocatalytic activity of our sample follows the same trend like the specific surface area.

As a whole, it can be concluded that annealing temperatures show significant effects on the surface specific activities of ZnO nanorods. Since the crystalline phase and exposed facets are kept unchanged during the different annealing temperature, the activity differences should originate from the different aspect ratio and defects. It is well known that the photocatalytic process is determined by the separation of electron/hole pairs (e^-/h^+)[41], and the separation of photogenerated carriers could be due to the crystalline phase, aspect ratio of nanorods, electronic structure of the facets and defects[42]. Among these factors, surface defects have to be considered for most cases except for perfect single crystals. Because the present ZnO nanorods were synthesized via a mechanical-assisted thermal decomposition method at relatively low temperature (350–500°C), diffusion length of atoms during decomposition reaction of the precursor is relatively short. It is therefore reasonable to believe that large number of surface defects exist in the final products, which result in visible emission (400–700 nm).

Generally recombination probability of the photogenerated carriers would be high, separation of electron-hole is the rate limiting step for the photocatalytic process[41]. The aspect ratio and electronic structure of the facets[41,42] are expected to enhance the separation of photogenerated carriers. Thus decreased recombination centers with less number of interparticle junctions and high electron delocalization in high aspect ratio nanorods leads to higher efficiency. Under the light irradiation, electron transfer from valance band to conduction band with the absorption of photo energy and electron-hole

pairs are then created on ZnO. In the case of a ZnO crystal free of any defects, the photogenerated electrons and holes undergo quick recombination both in the bulk phase and on the surface. In the case of ZnO with defects, the circumstances are a bit more complicated. The photogenerated holes can be trapped by surface defects, i.e. defect clusters, and the separation of photogenerated electron-hole pairs is facilitated. Moreover, the photogenerated holes trapped by surface defects are ready to react with electron donors and the photocatalytic reaction can be greatly promoted. Obviously, the existence of surface defects plays a positive role in the photocatalytic activity of ZnO nanorods. However, XPS and PL results are not suitable for the quantitative analysis of surface defects, so it should be mentioned that we could not correlate the photocatalytic activity with surface defects. Further experiments are therefore needed in order to address the correlation between defect and photocatalytic activity.

For 1-D nanostructured crystals the space charge region is well constructed along the longitudinal direction of ZnO nanocrystal, meaning that photogenerated electrons can flow in the direction of the crystal length. Increased delocalization of electrons at 1-D nanostructured crystals can lead to a remarkable decrease in e^-/h^+ recombination probability. Consequently, larger number of e^- and h^+ exist on the active sites of the nanocrystal surface, resulting in higher activity compared with spherical nanoparticles. In the previous study, Yun et al.[43] reported that decreased recombination centers with less number of interparticle junctions leads to higher efficiency. Therefore, the present data implies that higher aspect ratio of ZnO nanorods with higher level of surface defect leads to greater photocatalytic activity, and these results indicate that ZnO nanorods with high-level defect of ZnO nanorods could be synthesized by using this modified thermal decomposition method.

In summary, four kinds of aspect ratio ZnO nanostructures were prepared by a simple mechanical-assisted thermal decomposition method at various temperatures. The photocatalytic studies showed that as-synthesized ZnO nanorods have good photocatalytic performance, and the photocatalytic activity increased with increasing aspect ratio. Characterization results from photoluminescence and XPS spectra indicate the existence of defects in ZnO nanorods. Moreover, the high aspect ratio of ZnO nanorods exhibit high level of surface defects, and high aspect ratio of ZnO nanorods with high level of surface defects are responsible for the high photocatalytic performance. This method is commercially gainful, easily producible for large quantity of catalyst and the necessity of special equipment is unessential.

Methods

Chemicals. Zinc acetate dihydrate (Carlo) used in the present study was of analytical reagent grade. Methylene blue (MB) was from Aldrich chemicals. All aqueous solutions were prepared using double distilled water.

Sample preparation. ZnO nanorods were synthesized by grinding 5.0 g of zinc acetate dihydrate without additive in a mortar for 30 min and then annealed in an alumina crucible at different temperature for 3 h, which is similar to the previous work. In the present study, the annealing temperature was 350°C, 400°C, 450°C, and 500°C for 3 h. After reaction, the powder was washed with distilled water twice and dried in an oven at 90°C for 8 h. The obtained samples were denoted as 350, 400, 450, and 500 according to the calcinations temperature.

Materials characterization. Powder X-ray diffraction (XRD) was carried out using Phillips X'pert diffractometer using Cu Kα radiation. Equipped with X'celerator detector and the instrument were operated at 40 kV and 25 mA. The 2θ range of 20–90° scanning was performed with a step size of 0.02, time per step is 4 s. Field emission scanning electron microscopy (FESEM) images were taken using Hitachi S-4700. Transmission electron microscopy (TEM) images were acquired with a JEM-2010 operated at 200 kV at Yanshan University. The samples were prepared by drop casting a sample dispersed in ethanol on carbon coated Cu-grids and dried in a vacuum. The thermal analysis was carried out using NETZSCH STA 409 simultaneous thermal analyzer and the photocatalytic activity was measured by Perkin-Elmer UV-vis spectrometer. X-ray photoelectron spectra (XPS) of the samples were recorded on XPS ESCA Thermo Fischer Scientific Multilab 2000 using monochromatic Al Kα radiation. Binding energies were corrected with respect to graphitic carbon at 284.6 eV. The surface area was determined by Brunauer-Emmett-Teller (BET) method using ASAP 2020 HD88 surface area and porosity analyzer. The photoluminescence (PL) excitation/emission measurements were performed on a Jobin-Yvon Nanolog-3 spectrofluorometer at room temperature. In all cases, the samples were excited by a 325 nm Xenon laser beam through optical lens. The excitation wavelength scanned from 350 to 700 nm with 5 nm steps for both samples.

Photocatalytic measurements. The photocalytic activity of ZnO nanorods with different aspect ratio was estimated by measuring the decomposition rate of MB aqueous solution under high-pressure sodium lamp (400 W, Philips, 400–650 nm) irradiation. In order to maintain the MB solution temperature at room temperature (35°C), water was circulated through the outside of the reactor. Reaction suspensions were prepared by adding the 250 mg of ZnO nanorods in 500 mL of aqueous MB solution taken with an initial concentration of 5 mg/L. The solution mixture was stirred for 2 h in dark to attain equilibrium adsorption. Experiments showed that no degradation occurred in the presence of catalyst without light. The aqueous suspension containing MB and the photocatalyst was irradiated with constant stirring. The analytical samples from the suspension were collected at regular intervals of time, centrifuged and filtered. The concentration of MB in each sample was analyzed using UV-vis spectrophotometer (Shimadzu, 1700 UV-VIS) at a wavelength of 664 nm. The photocatalytic efficiency was calculated using the expression $\eta = (1 - C/C_0)*100$, where C_0 is the concentration of MB before illumination and C is the concentration after irradiation time.

1. Ferrando, R., Jellinek, J. & Johnston, R. L. Nanoalloys: from theory to applications of alloy clusters and nanoparticles. *Chem. Rev.* **108**, 845–910 (2008).
2. Fernández-García, M., Martínez-Arias, A., Hanson, J. C. & Rodriguez, J. A. Nanostructured Oxides in Chemistry: Characterization and Properties. *Chem. Rev.* **104**, 4063–4104 (2004).
3. Talapin, D. V., Lee, J.-S., Kovalenko, M. V. & Shevchenko, E. V. Prospects of Colloidal Nanocrystals for Electronic and Optoelectronic Applications. *Chem. Rev.* **110**, 389–458 (2009).
4. Reynolds, D. C. *et al.* Time-resolved photoluminescence lifetime measurements of the Γ5 and Γ6 free excitons in ZnO. *J. Appl. Phys.* **88**, 2152 (2000).
5. Lim, J. H. *et al.* UV Electroluminescence Emission from ZnO Light-Emitting Diodes Grown by High-Temperature Radiofrequency Sputtering. *Adv. Mater.* **18**, 2720–2724 (2006).
6. Lansdown, A. B. G. & Taylor, A. Zinc and titanium oxides: promising UV-absorbers but what influence do they have on the intact skin? *Int. J. Cosmet. Sci.* **19**, 167–172 (1997).
7. Mohammad, M. T., Hashim, A. A. & Al-Maamory, M. H. Highly conductive and transparent ZnO thin films prepared by spray pyrolysis technique. *Mater. Chem. Phys.* **99**, 382–387 (2006).
8. Becker, J., Raghupathi, K. R., St. Pierre, J., Zhao, D. & Koodali, R. T. Tuning of the Crystallite and Particle Sizes of ZnO Nanocrystalline Materials in Solvothermal Synthesis and Their Photocatalytic Activity for Dye Degradation. *J. Phys. Chem. C* **115**, 13844–13850 (2011).
9. Ali, A. M., Emanuelsson, E. A. C. & Patterson, D. A. Photocatalysis with nanostructured zinc oxide thin films: The relationship between morphology and photocatalytic activity under oxygen limited and oxygen rich conditions and evidence for a Mars Van Krevelen mechanism. *Appl. Catal., B.* **97**, 168–181 (2010).
10. Wang, J. *et al.* Relationship between Oxygen Defects and the Photocatalytic Property of ZnO Nanocrystals in Nafion Membranes. *Langmuir.* **25**, 1218–1223 (2008).
11. McLaren, A., Valdes-Solis, T., Li, G. & Tsang, S. C. Shape and Size Effects of ZnO Nanocrystals on Photocatalytic Activity. *J. Am. Chem. Soc.* **131**, 12540–12541 (2009).
12. Jang, E. S., Won, J. H., Hwang, S. J. & Choy, J. H. Fine Tuning of the Face Orientation of ZnO Crystals to Optimize Their Photocatalytic Activity. *Adv. Mater.* **18**, 3309–3312 (2006).
13. Tian, Z. R. *et al.* Complex and oriented ZnO nanostructures. *Nat. Mater.* **2**, 821–826 (2003).
14. Wang, L. *et al.* Systematic Investigation on Morphologies, Forming Mechanism, Photocatalytic and Photoluminescent Properties of ZnO Nanostructures Constructed in Ionic Liquids. *Inorg. Chem.* **47**, 1443–1452 (2008).
15. Zhang, L. *et al.* Controllable synthesis and shape-dependent photocatalytic activity of ZnO nanorods with a cone and different aspect ratios and of short-and-fat ZnO microrods by varying the reaction temperature and time. *Appl. Phys. A.* **100**, 1061–1067 (2010).
16. McLaren, A., Valdes-Solis, T., Li, G. & Tsang, S. C. Shape and Size Effects of ZnO Nanocrystals on Photocatalytic Activity. *J. Am. Chem. Soc.* **131**, 12540–12541 (2009).
17. Dodd, A., McKinley, A., Tsuzuki, T. & Saunders, M. Tailoring the photocatalytic activity of nanoparticulate zinc oxide by transition metal oxide doping. *Mater. Chem. Phys.* **114**, 382–386 (2009).
18. Guo, M. Y. *et al.* Effect of Native Defects on Photocatalytic Properties of ZnO. *J. Phys. Chem. C* **115**, 11095–11101 (2011).
19. Wang, J.-L., Wang, J.-Q., He, L.-N., Dou, X.-Y. & Wu, F. A CO2/H2O2-tunable reaction: direct conversion of styrene into styrene carbonate catalyzed by sodium phosphotungstate/n-Bu4NBr. *Green Chem.* **10**, 1218–1223 (2008).

20. Zheng, Y. *et al*. Luminescence and Photocatalytic Activity of ZnO Nanocrystals: Correlation between Structure and Property. *Inorg. Chem.* **46**, 6675–6682 (2007).
21. Kong, M. *et al*. Tuning the Relative Concentration Ratio of Bulk Defects to Surface Defects in TiO2 Nanocrystals Leads to High Photocatalytic Efficiency. *J. Am. Chem. Soc.* **133**, 16414–16417 (2011).
22. Lin, C.-C. & Li, Y.-Y. Synthesis of ZnO nanowires by thermal decomposition of zinc acetate dihydrate. *Mater. Chem. Phys.* **113**, 334–337 (2009).
23. Saravanan, R., Shankar, H., Prakash, T., Narayanan, V. & Stephen, A. ZnO/CdO composite nanorods for photocatalytic degradation of methylene blue under visible light. *Mater. Chem. Phys.* **125**, 277–280 (2011).
24. Mishra, S. K., Srivastava, R. K. & Prakash, S. G. ZnO nanoparticles: Structural, optical and photoconductivity characteristics. *J. Alloy. Compd.* **539**, 1–6 (2012).
25. Saravanan, R. *et al*. ZnO/Ag nanocomposite: An efficient catalyst for degradation studies of textile effluents under visible light. *Mater. Sci. Eng. C* **33**, 2235–2244 (2013).
26. Liu, J.-s., Cao, J.-m., Li, Z.-q., Ji, G.-b. & Zheng, M.-b. A simple microwave-assisted decomposing route for synthesis of ZnO nanorods in the presence of PEG400. *Mater. Lett.* **61**, 4409–4411 (2007).
27. Bhatkhande, D. S., Pangarkar, V. G. & Beenackers, A. A. C. M. Photocatalytic degradation for environmental applications – a review. *J. Chem. Technol. Biotechnol.* **77**, 102–116 (2002).
28. Orel, Z. C., Gunde, M. K. & Orel, B. Application of the Kubelka-Munk theory for the determination of the optical properties of solar absorbing paints. *Prog. Org. Coat.* **30**, 59–66 (1997).
29. Madhusudan Reddy, K., Manorama, S. V. & Ramachandra Reddy, A. Bandgap studies on anatase titanium dioxide nanoparticles. *Mater. Chem. Phys.* **78**, 239–245 (2003).
30. Zhang, H., Lu, S., Xu, W. & Yuan, F. First-principles study of electronic structures and photocatalytic activity of low-Miller-index surfaces of ZnO. *J. Appl. Phys.* **113**, 034903–034908 (2013).
31. Lakshmi, S., Renganathan, R. & Fujita, S. Study on TiO2-mediated photocatalytic degradation of methylene blue. *J. Photochem. Photobiol. A* **88**, 163–167 (1995).
32. Shu, X., He, J., Chen, D. & Wang, Y. Tailoring of Phase Composition and Photoresponsive Properties of Ti-Containing Nanocomposites from Layered Precursor. *J. Phys. Chem. C* **112**, 4151–4158 (2008).
33. Zheng, J. H., Jiang, Q. & Lian, J. S. Synthesis and optical properties of flower-like ZnO nanorods by thermal evaporation method. *Appl. Surf. Sci.* **257**, 5083–5087 (2011).
34. Han, X.-G. *et al*. Controlling Morphologies and Tuning the Related Properties of Nano/Microstructured ZnO Crystallites. *J. Phys. Chem. C* **113**, 584–589 (2008).
35. Iwabuchi, A., Choo, C.-k. & Tanaka, K. Titania Nanoparticles Prepared with Pulsed Laser Ablation of Rutile Single Crystals in Water. *J. Phys. Chem. B* **108**, 10863–10871 (2004).
36. Wang, R., Sakai, N., Fujishima, A., Watanabe, T. & Hashimoto, K. Studies of Surface Wettability Conversion on TiO2 Single-Crystal Surfaces. *J. Phys. Chem. B* **103**, 2188–2194 (1999).
37. Cong, Y., Zhang, J., Chen, F. & Anpo, M. Synthesis and Characterization of Nitrogen-Doped TiO2 Nanophotocatalyst with High Visible Light Activity. *J. Phys. Chem. C* **111**, 6976–6982 (2007).
38. Djurišić, A. B. *et al*. Photoluminescence and Electron Paramagnetic Resonance of ZnO Tetrapod Structures. *Adv. Funct. Mater.* **14**, 856–864 (2004).
39. Wang, J., Li, Q., Peng, L. & Malac, M. Electron Energy Loss Spectroscopy Study on the Dielectric Response of Single H2Ti3O7 Nanotube. *Microsc. Microanal.* **15**, 1218–1219 (2009).
40. Liu, S., Li, C., Yu, J. & Xiang, Q. Improved visible-light photocatalytic activity of porous carbon self-doped ZnO nanosheet-assembled flowers. *CrystEngComm* **13**, 2533–2541 (2011).
41. Herrmann, J. M. Heterogeneous photocatalysis: state of the art and present applications In honor of Pr. R. L. Burwell Jr. (1912–2003), Former Head of Ipatieff Laboratories, Northwestern University, Evanston (Ill). *Top. Catal.* **34**, 49–65 (2005).
42. Chang, J. & Waclawik, E. R. Facet-controlled self-assembly of ZnO nanocrystals by non-hydrolytic aminolysis and their photodegradation activities. *CrystEngComm* **14**, 4041–4048 (2012).
43. Yun, H. J., Lee, H., Joo, J. B., Kim, W. & Yi, J. Influence of Aspect Ratio of TiO2 Nanorods on the Photocatalytic Decomposition of Formic Acid. *J. Phys. Chem. C* **113**, 3050–3055 (2009).

Acknowledgments

This work was supported by the Ratchadaphiseksomphot Endowment Fund of Chulalongkorn University (RES560530022-AM), NBRPC (grant 2013CB733000), NSFC (grants 51271161/51171160/51002130/51171163). The authors would like to acknowledge support from Chulalongkorn University (GDNS 56-010-62-001) and Key Laboratory of Metastable Materials Science and Technology, Yanshan University.

Author contributions

J.Q. and X.Z. designed and coordinated the overall study. J.Q., X.Z., Y.X., P.Y., B.Z., L.W. and R.L. performed experiments and analyzed data. J.Q. and X.Z. wrote the manuscript. All authors discussed the results and commented on the manuscript.

Additional information

Competing financial interests: The authors declare no competing financial interests.

How to cite this article: Zhang, X.Y. *et al*. Effect of aspect ratio and surface defects on the photocatalytic activity of ZnO nanorods. *Sci. Rep.* **4**, 4596; DOI:10.1038/srep04596 (2014).